# Quantized escape and formation of edge channels at high Landau levels and edge transport mediated zero-differential resistance states

A. D. Chepelianskii,[1,2] J. Laidet,[2] I. Farrer,[1] D. A. Ritchie,[1] K. Kono,[3] and H. Bouchiat[2]
[1]*Cavendish Laboratory, University of Cambridge, J J Thomson Avenue, Cambridge CB3 OHE, United Kingdom*
[2]*LPS, Université Paris-Sud, CNRS, UMR 8502, F-91405 Orsay, France*
[3]*Low Temperature Physics Laboratory, RIKEN, Wako, Saitama 351-0198, Japan*
(Received 1 April 2014; revised manuscript received 2 June 2014; published 2 July 2014)

We present nonlocal resistance measurements in an ultrahigh-mobility two-dimensional electron gas. Our experiments show that even at weak magnetic fields, classical guiding along edges leads to a strong nonlocal resistance on macroscopic distances. In this high Landau level regime, the transport along edges is dissipative and can be controlled by the amplitude of the voltage drop along the edge. We report resonances in the nonlocal transport as a function of this voltage that are interpreted as escape and formation of edge channels, and the formation of zero-differential resistance states when the nonlocal voltage is measured on length scales much larger than the mean free path.

DOI: 10.1103/PhysRevB.90.045301 PACS number(s): 73.40.−c, 05.45.−a, 72.20.My, 73.50.Jt

The investigation of nonlocal effects in electrical transport has provided new insights into nonclassical conduction mechanisms. These effects are responsible for the appearance of a potential difference across a region of the sample well outside of the classical current paths. They have been reported in conductors that exhibit quantum coherence [1–3], ballistic transport [4,5], or in the quantum Hall effect regime of a two-dimensional electron gas [6–8]. In the latter case, the nonlocal resistance appears due to the formation of edge channels that are isolated from the bulk and can carry the current to classically inaccessible regions. The propagation of edge channels in this regime has attracted a significant interest due to their potential for quantum computation and interferometry [9–12]. Here, using nonlocal measurements, we consider the opposite limit of high Landau levels where the bulk density of states is gapless. We show that in this limit, the exchange of charges between bulk and edge states can be controlled by the voltage drop along the edges, which leads to the formation of resonances in the nonlinear transport that allow us to observe directly a quantization of edge channels at high Landau levels. Our results are also important for the understanding of nonequilibrium physics in ultrahigh-mobility two-dimensional electron gases (2DEGs), which has attracted significant attention recently in connection with the discovery of microwave-induced zero-resistance states [13–27] (for a review, see [28]). Indeed, we also demonstrate that edge transport phenomena can lead to the formation of zero-differential resistance states very similar to those reported in Hall-bar and Corbino-disk measurement geometries [29–31]. These findings support the importance of edge transport in the understanding of the unexpected transport properties of 2DEGs far from equilibrium [32–36].

We start by describing the measurement geometry for nonlocal magnetoresistance and by explaining the results we obtained in the linear regime. We then focus on the nonlinear regime at larger polarization currents, showing the appearance of spectacular resonances in the nonlocal differential resistance, which we interpret as a manifestation of the quantized escape and formation of edge channels. Finally, we demonstrate that these resonances can give rise to zero-differential resistance states when the nonlocal resistance is probed in a macroscopic measurement geometry where all the length scales are larger than the mean free path, effectively averaging to zero the nonlocal differential resistance.

## I. NONLOCAL MAGNETOTRANSPORT IN THE LINEAR REGIME

We have investigated the magnetic-field dependence of nonlocal transport in a GaAs/$Ga_{1-x}Al_xAs$ 2DEG with density $n_e \simeq 3.3\times10^{11}$ cm$^{-2}$, mobility $\mu \simeq 10^7$ cm$^2$/V s corresponding to transport time $\tau_{tr} \simeq 0.4$ ns, and a mean free path of $\ell_e = 100$ $\mu$m. The Hall bar with a channel width $W = 100$ $\mu$m was patterned using wet etching. The nonlocal resistance $R_{nl}$ was measured in a geometry illustrated in Fig. 1 where current was injected along the $y$ axis and the voltage was detected between two probes distant by $D_x \simeq 50$ $\mu$m at a distance $L \gg W$ from the current injection points. The experimental data in Fig. 2 show that $R_{nl}$ exhibits an unusual dependence on magnetic field that is strikingly different from $\rho_{xx}$ behavior. Indeed, in contrast to $\rho_{xx}(B)$, $R_{nl}(B)$ is a strongly asymmetric function of the magnetic field that almost vanishes for negative magnetic fields and exhibits a sharp onset at low positive magnetic fields reaching a value of the order of $\rho_{xx}$ for $B > 0.1$ T.

We have first checked whether this dependence can be explained using the continuum theory of a Hall bar. For this purpose, it is convenient to describe our sample as a 2DEG stripe, and to approximate the current injection leads by pointlike sources. This stripe can be parametrized by complex numbers $z = x + iy$ with $y \in (0,W)$. The potential $V(z)$ created by a current source $I$ positioned at $x = x_0$ along the top and bottom edges then reads $V_\pm(z) = R_\pm(z,x_0)I$ [plus (minus) sign for top (bottom) edge], where

$$R_\pm(z,x_0) = R_p\left[\exp\left(\frac{\pi z}{W}\right)\exp\left(\frac{-\pi x_0}{W}\right) \pm 1\right]. \quad (1)$$

The function $R_p$ gives the potential created by a unit current source located at the origin in the semi-infinite 2DEG

 

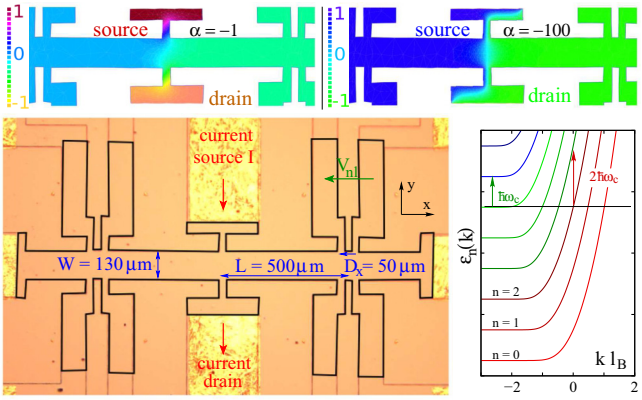


FIG. 1. (Color online) Sample geometry in our nonlocal transport experiments. Arrows indicate the geometrical parameters in our experiment, the position of the source and drain electrodes, and the electrodes across which the nonlocal potential drop $V_{nl}$ is measured. The nonlocal resistance is then defined as $R_{nl} = V_{nl}/I$. The closed black contour highlights the geometry of the domain used in our finite-element simulations whose results are displayed in the top panels for $\alpha = \rho_{xy}/\rho_{xx} = -1$ and $\alpha = -100$, the color (gray-scale) level indicates the potential values [source (drain) potentials are fixed to $\pm 1$]; the potential gradients are concentrated in the center of the sample. The curves on the right represent the dispersion relation $\epsilon_n(k)$ for edge states for a hard wall potential, $k$ is the wave number, and $l_B$ is the magnetic length [37].

half-plane $y > 0$:

$$R_p(z) = \frac{\rho_{xx}}{\pi}(\log|z| + \alpha \arg z), \tag{2}$$

where we introduced the notation $\alpha = \rho_{xy}/\rho_{xx}$.

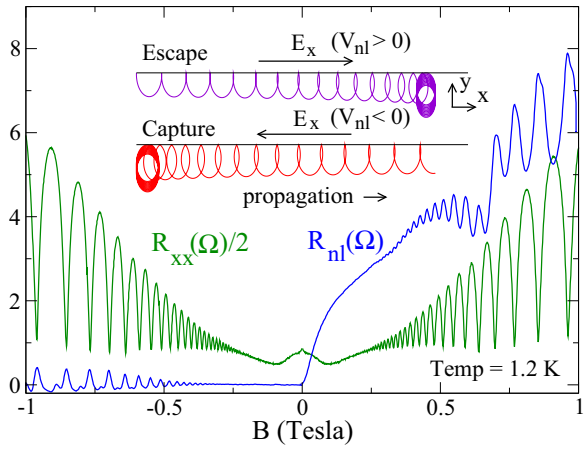


FIG. 2. (Color online) Dependence of the nonlocal resistance $R_{nl}$ (as defined in Fig. 1) and of the longitudinal resistance $R_{xx} \simeq \rho_{xx}$ on the magnetic field $B$. The longitudinal resistance $R_{xx}$ is almost a symmetric function of $B$, whereas $R_{nl}(B)$ is strongly asymmetric and almost vanishes for $B < 0$. The insets illustrate typical classical electron orbits for a capture and an escape event due to the parallel electric field $E_x$ for $B > 0$, where electrons propagate along the upper edge in the positive $x$ direction. Capture occurs for $V_{nl} < 0$ and escape occurs for $V_{nl} > 0$.

Subtracting these two expressions, we find the potential $V = [R_+(z,0) - R_-(z,0)]I$ created by a current between a pointlike source and drain located opposite to each other along the channel. Using these equations for the particular case of the potential generated along the top edge $z = iW$, far from the sources $|x| \gg W$, we find the following expression for the nonlocal resistance:

$$R_{nl} = \frac{2\rho_{xx}D_x}{W}\exp\left(-\frac{\pi L}{W}\right), \tag{3}$$

where $D_x$ is the spacing between the voltage probes and $L$ is their distance from the source along the channel (for simplicity, we have assumed $D_x \ll W$). The geometrical parameters in our experiment are $L \simeq 500\ \mu$m, $W \simeq 130\ \mu$m, and $D_x \simeq 50\ \mu$m (see Fig. 1), which lead to a numerical estimation $R_{nl} \simeq 4.4\times10^{-6}\rho_{xx}$. Thus according to this point source model, the nonlocal resistance is proportional to $\rho_{xx}$ with an exponentially small damping factor that is independent of the magnetic field. This conclusion, however, is in strong disagreement with the experimentally observed dependence. To check the validity of this analytical estimation in our more complex experimental geometry, we have performed a finite-element simulation of the potential that (see Fig. 1) confirms the exponential decay of the field amplitudes away from the current polarization contacts.

Thus even at small magnetic fields ($\leqslant$0.1 T), our experiments indicate a large nonlocal resistance that cannot be described within the continuum theory. Due to the macroscopic dimensions of our sample (channel width $W \simeq 130\ \mu$m), quantum coherence effects cannot explain the origin of the nonlocal resistance in our measurements. An explanation relying solely on the formation of Landau levels is also unlikely since we observe $R_{nl} \sim \rho_{xx}$ even at weak magnetic fields $B \simeq 0.1$ T where Shubnikov–de Haas oscillations are absent. We thus propose guiding along sample edges as a possible explanation for the observed behavior, and we attempt to include the physics of skipping orbits within the continuum model. The formation of skipping orbits occurs due to the bending of the Landau levels at the edge of the 2DEG [37], which is represented in Fig. 2. It can lead to noticeable effects even when individual Landau levels are not resolved [38].

In the presence of skipping orbits, electrons can propagate along the edges before being injected into the bulk of the 2DEG. This gives rise to edge currents $I_+, I_-$ along the top and bottom edges of the sample. Due to the influence of disorder, electrons will progressively detach from the edges causing a progressive drop of the edge current in the direction of propagation of the electrons. The drop in the current carried by the edges $dI_+/dx$ and $dI_-/dx$ creates a distributed current source for the bulk of the 2DEG. Equation (1) derived within the continuum model allows us to find the potential created by this distributed current source:

$$V = -\int R_+(z,x)\frac{dI_+(x)}{dx}dx - \int R_-(z,x)\frac{dI_-(x)}{dx}dx. \tag{4}$$

We will assume that the edge currents are nonzero only in the direction of propagation of the electrons, and that they decay exponentially with a characteristic length scale $\lambda_e$ that we will

call the mean free path along edges. This leads to

$$I_+(x) = I_-(-x) = s_B I e^{-s_B x/\lambda_e}\eta(s_B x), \tag{5}$$

where $s_B = \pm 1$ for positive (negative) magnetic fields and $\eta$ is the Heaviside function. It is straightforward to check that the total current $-\int \frac{dI_+(x)}{dx}dx$ injected into the bulk 2DEG from the top electrode is $I$. Assuming $|\alpha| \gg 1$ and combining Eqs. (4) and (5), we find the following approximation for the nonlocal resistance:

$$R_{\rm nl} = \rho_{xy}\frac{W}{\lambda_e}\exp\left(-\frac{\pi L}{\lambda_e}\right)\eta(s_B). \tag{6}$$

Since this equation was derived assuming that electrons were guided only in one direction, it predicts a vanishing nonlocal resistance for negative magnetic fields, in qualitative agreement with the experiment. We note, however, that for $B < -0.5$ T, a finite nonlocal resistance of oscillating sign appears that is not expected within this model. A possible origin of this effect could be due to electrons that are recaptured by the edges after moving through the bulk of the samples and that are not accounted for in the present model. At positive magnetic fields, this equation can be used to estimate $\lambda_e$ from the experimental data, which yields for $B \geqslant 0.1$ T, $\lambda_e \simeq 90\ \mu$m. Weak variations of $\lambda_e$ as a function of the magnetic field (at most 10%) can explain the presence of Shubnikov–de Haas oscillations in $R_{\rm nl}(B)$. We note that the obtained value $\lambda_e$ is very close to the transport mean free path in the sample, $\ell_e \simeq 100\ \mu$m.

## II. SIGNATURE OF THE QUANTIZED ESCAPE AND FORMATION OF EDGE CHANNELS IN THE NONLINEAR TRANSPORT

Even if the proposed model describes qualitatively the observed nonlocal resistance, it is based on a phenomenological assumption on the distribution of the edge currents $I_e(x)$, and a microscopic theory is needed to determine self-consistently the potential inside the device and the distribution of the edge currents. Several approaches have been proposed to treat the interaction between bulk and edge transport in the quantum limit at low filling factors [6,39–41], but they do not directly apply to the present case. Indeed, the propagation along edge channels has mainly been studied at an integer quantum Hall effect plateau, where the transport is nondissipative, $R_{xx} = 0$, and a gap in the density of states opens in the bulk [10,12].

In our case, due to the low magnetic fields, the gap is not present and electrons can escape to the bulk or on the contrary approach toward the edge. To look for signatures of the escape and creation of edge channels, we have measured the nonlocal differential resistance (NLDR) $dV_{\rm nl}/dI$ as a function of magnetic field and dc excitation current $I$. At positive magnetic fields, when the potential $V_{\rm nl}$ is positive, electrons lose energy $|e|V_{\rm nl}$ as they cross the separation distance between the voltage probes, thus some electrons will escape from the edge because their Larmor radius becomes smaller as they propagate. If the potential $V_{\rm nl}$ is negative, electrons in the bulk will tend to drift toward the edge under the action of the electric field, $E_x = V_{\rm nl}/D_x$, and new edge channels may be formed. The typical trajectories for a capture and an escape event are represented in Fig. 2. We thus expect that the transport properties along the edge will depend strongly on the sign of $V_{\rm nl}$.

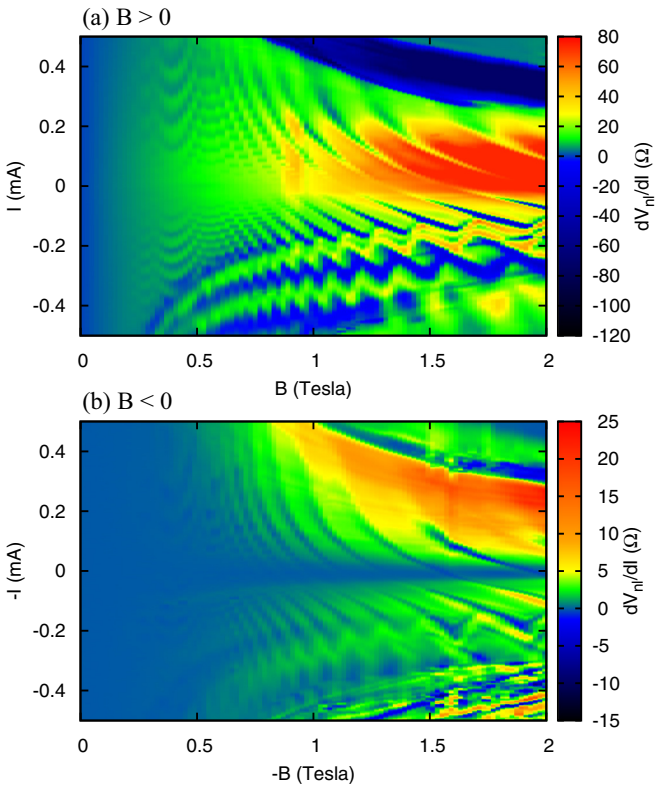


FIG. 3. (Color online) Dependence of the differential nonlocal resistance $dV_{\rm nl}/dI$ on magnetic field $B$ and on the dc current amplitude $I$ for positive and negative magnetic fields (top and bottom panels, respectively). The data at negative magnetic fields are displayed as a function of $-B$ and $-I$. Temperature was 1.2 K.

In agreement with our heuristic arguments, the experimental results displayed in Fig. 3 exhibit a striking asymmetry between positive and negative currents. For positive currents (at $B \geqslant 0.5$ T), we measure positive $dV_{\rm nl}/dI$ for $I > 0$, whereas for $I < 0$, $dV_{\rm nl}/dI$ drops and exhibits sharp oscillations around zero. To ensure that this difference is not related to some asymmetry of the sample, we have also measured $dV_{\rm nl}/dI$ at negative magnetic fields. Except for the region around $I = 0$ where the differential resistance almost vanishes, in agreement with our guiding model, we find that after the transformation $I \to -I$, results are very similar to those obtained at $B > 0$. This observation confirms that our findings cannot be attributed to a geometrical asymmetry which would not depend on the sign of the magnetic field. To understand the origin the approximate symmetry observed in Fig. 3, we note that a mirror symmetry around the Hall bar channel changes, $I \to -I$ and $B \to -B$, and interexchanges top and bottom edges. The nonlocal voltage across the bottom edge is therefore expected to be $V_{\rm nl}(-B, -I)$, and the electrons emitted from the bottom edge can then be recaptured at the top edge where $dV_{\rm nl}/dI$ is measured, giving a contribution proportional to $dV_{\rm nl}/dI$ at $B > 0$ and current $-I$ damped by the propagation through the bulk. Hence from now on we will focus on the analysis of the data obtained at $B > 0$.

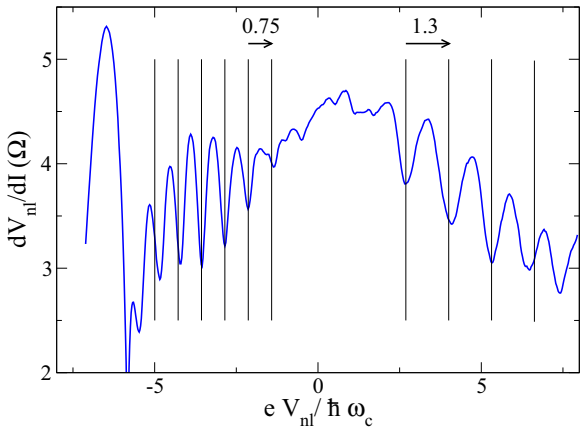


FIG. 4. (Color online) Dependence of the differential nonlocal resistance $dV_{\rm nl}/dI$ on the dimensionless quantity $eV_{\rm nl}/\hbar\omega_c$ at a magnetic field of 0.3 T. The vertical lines on the left and right are equally spaced with respective spacing 0.75 and 1.3, and they are a guide to the eye to show the periodicity of the oscillations.

The dependence on $I$ displayed in Fig. 3 exhibits several intriguing features. To gain an understanding of their physical origin, we will concentrate on the region of weak magnetic fields ($B$ between 0.2 and 0.9 T). In this region, $dV_{\rm nl}/dI$ exhibits smooth oscillations as a function of $I$. Integrating on current, we find the dependence $V_{\rm nl}(I)$ and display the differential resistance as a function of $eV_{\rm nl}/\hbar\omega_c$, where $\hbar\omega_c$ is the spacing between Landau levels. This transformation reveals the periodic nature of the observed NLDR oscillations. An example of the experimental dependence of NLDR as a function of $eV_{\rm nl}/\hbar\omega_c$ at $B = 0.3$ T is shown in Fig. 4, and several oscillations are resolved at both positive and negative voltages, which allows us to define with good accuracy the period $\Delta V_{\rm nl}$ of the oscillations. We note that at $B = 0.3$ T, the amplitude of the Shubnikov–de Haas oscillations on the longitudinal resistance $R_{xx}$ represents around 15% of the total magnetoresistance (see Fig. 2). This corresponds to a low magnetic field regime where there is no energy gap in the bulk density of states.

The dependence of the oscillation period $\Delta V_{\rm nl}$ on the magnetic field is displayed in the inset of Fig. 5. As shown in Fig. 5, at higher magnetic fields, $B \geqslant 0.6$ T, only a limited number of oscillations can be resolved. In those cases, we use the distance between the first resolved peaks to define $\Delta V_{\rm nl}$. For $V_{\rm nl} < 0$, where we expect the formation of new edge channels due to drift of bulk electrons toward the edge, $\Delta V_{\rm nl}$ is almost equal to $\hbar\omega_c/e$ (we attribute the 20% difference to the aspect ratio between the distance between voltage probes and their width). However, for $V_{\rm nl} > 0$, when electrons lose energy as they propagate and edge channels progressively escape to the bulk, the ratio $e\Delta V_{\rm nl}/\hbar\omega_c$ progressively increases with magnetic field. Our interpretation is that at $V_{\rm nl} < 0$, we are probing the outermost edge channels that have an energy spacing close to $\hbar\omega_c$, while for $V_{\rm nl} > 0$ edge channels escape progressively and only the inner channels with an energy spacing larger than $\hbar\omega_c$ are still propagating (see the level diagram in Fig. 1).

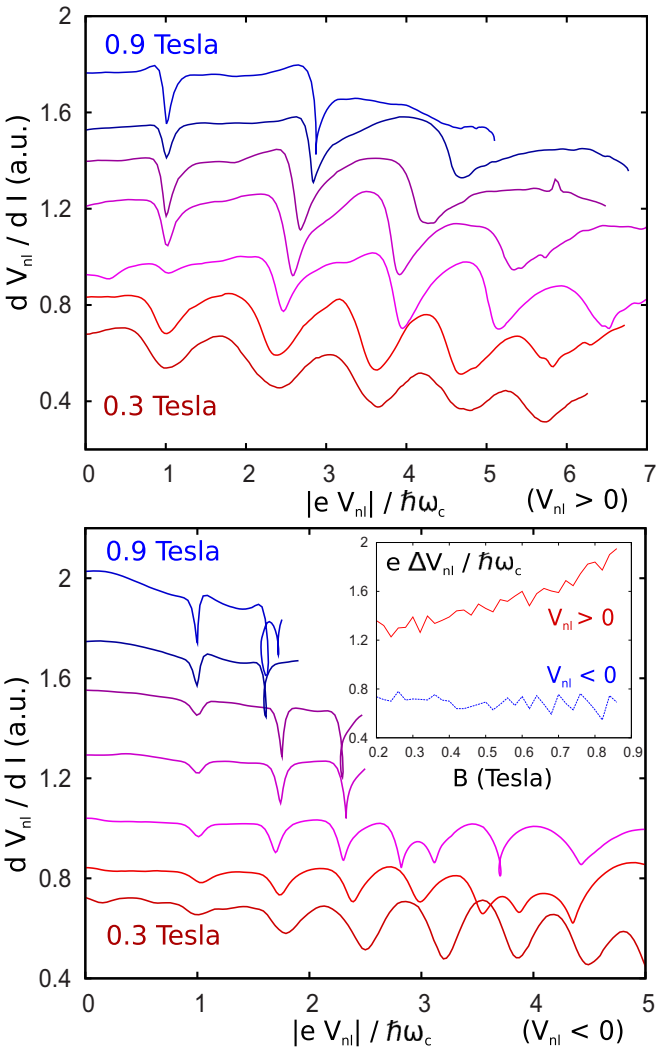


FIG. 5. (Color online) Dependence of the differential nonlocal resistance $dV_{\rm nl}/dI$ (in arbitrary units) on the dimensionless quantity $x = |eV_{\rm nl}|/\hbar\omega_c$ at magnetic fields between 0.3 and 0.9 T. A voltage offset was applied to fix the position of the first resolved peak at $x = 1$. The period of the oscillations is plotted as a function of magnetic field in the inset for positive and negative $V_{\rm nl}$. It corresponds to the distance between the first resolved peaks at magnetic fields where only a few oscillations could be resolved.

As the magnetic field increases, the following trends can be noted: for $I > 0$, the smooth oscillations develop into sharp resonances at certain values of $V_{\rm nl}$, while for negative currents, $dV_{\rm nl}/dI$ starts to change sign as a function of $I$, rendering our analysis as a function of $V_{\rm nl}$ impossible. Experiments with a larger separation between voltage probes, $D_x \simeq 500$ $\mu$m, did not display the described oscillation and resonances, which suggests that their observation is possible only when $D_x$ is smaller than the mean free path. In a control sample with wide voltage probes of around 300 $\mu$m, a zero-differential resistance plateau was observed at $I < 0$, indicating that in this regime the electrostatic potential oscillates as a function of the distance along the edge and averages to zero when the voltage is measured on a large length scale. These experimental results are described in detail in the next section.

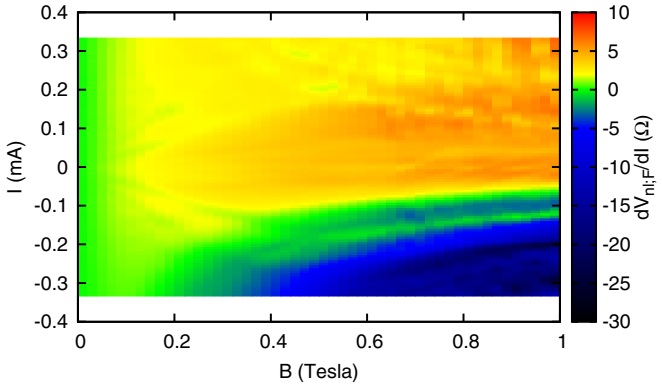


FIG. 6. (Color online) Dependence of the nonlocal differential resistance $dV_{\mathrm{nl};F}/dI$ on magnetic field and dc current amplitude; this quantity was measured in a geometry where the separation between voltage probes was $D_x \simeq 500\ \mu$m on the $\mu = 10^7\ \mathrm{cm}^2/\mathrm{V\,s}$ sample from the first two sections. The size of the voltage probe contacts on the Hall probe is still smaller than the mean free path, with a lateral dimension of around 10 $\mu$m, as can be seen on the optical image of the sample on Fig. 1. Temperature was $T = 1.2$ K.

## III. TRANSITION TO ZERO-DIFFERENTIAL RESISTANCE STATES IN MACROSCOPIC GEOMETRIES

A vanishing differential resistance has previously been reported in local measurement geometries [29–31] where bulk and edge contributions are intermixed. Our experiments show that a zero-differential resistance state can be created by edge effects alone.

We have measured NLDR in a geometry where the voltage probes were separated by a distance $D_x = 500\ \mu$m larger than the mean free path $\ell_e = 100\ \mu$m in the sample. The experiment was performed on the same sample but with a different arrangement of voltage and current probes, and the current sources were located 500 $\mu$m away from the voltage probes. We designate the signal measured in this geometry as $dV_{\mathrm{nl};F}/dI$. In the linear-response regime, the dependence of $R_{\mathrm{nl};F} = dV_{\mathrm{nl};F}/dI(I = 0)$ on the magnetic field was very similar to the data shown in Fig. 2. The quantity $R_{\mathrm{nl};F}$ was finite for positive magnetic fields and almost vanished for $B < 0$. The dependence of $dV_{\mathrm{nl};F}/dI$ on the magnetic field $B$ and on the dc current amplitude $I$ is represented in Fig. 6 for $B > 0$. The oscillating features as a function of the dc current $I$ are not resolved, contrary to measurements where $D_x$ was smaller than the mean free path (see the data in Fig. 3). Negative values of $dV_{\mathrm{nl};F}/dI$ at negative current $I$ are still observed in this geometry.

We have also studied NLDR in a macroscopic geometry with all the geometrical parameters larger than the mean free path. In this sample, the size of the voltage probes was much larger than the mean free path as opposed to the voltage probe configuration in the experiment shown in Fig. 6. The sample was made in a lower mobility 2DEG, with mobility $\mu = 3\times10^6\ \mathrm{cm}^2/\mathrm{V\,s}$ and a carrier density of $n_e = 3.2\times10^{11}\ \mathrm{cm}^{-2}$. The geometry of the measurement is sketched in Fig. 7. This figure summarizes our results on the NLDR in this sample, for positive magnetic fields for which the nonlocal resistance is nonvanishing.

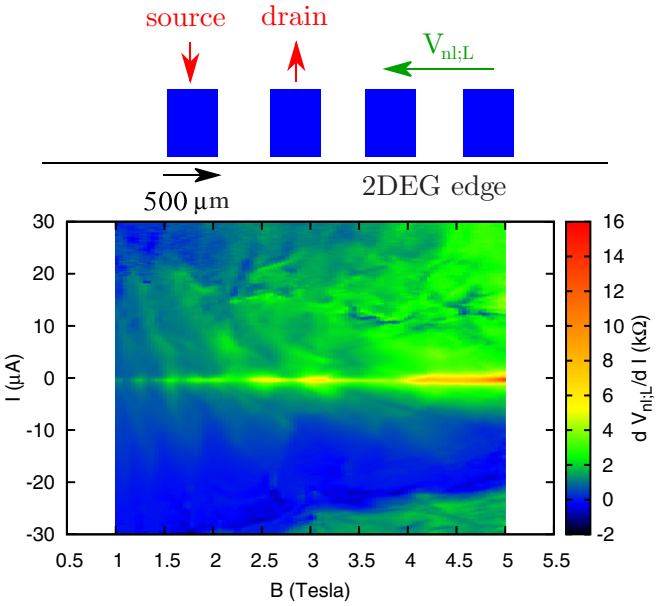


FIG. 7. (Color online) Dependence of NLDR $dV_{\mathrm{nl};L}/dI$ on magnetic field and dc current amplitude for the $\mu = 3\times10^6\ \mathrm{cm}^2/\mathrm{V\,s}$ mobility sample. NLDR was measured in the geometry sketched in the top panel. In this geometry, the distance between the voltage probes and the voltage probe size were both significantly larger than the mean free path with dimensions around 500 $\mu$m. Temperature was $T = 0.3$ K.

The strong asymmetry between positive and negative currents is also observed in this lower-mobility 2DEG, however the characteristic magnetic field where the asymmetry appears is around a factor 3 stronger as compared to the $\mu = 10^7\ \mathrm{cm}^2/\mathrm{V\,s}$ sample. This difference is consistent with the ratio between the mobilities of the two samples. As in Fig. 6, the separation between the voltage probes was larger than the mean free path, $\ell_e = 30\ \mu$m, and the oscillations as a function of the dc current cannot be resolved. However, in the present experiment, NLDR is almost zero in a large region of negative currents, which contrasts with previous data where NLDR could be negative for $I < 0$ (see Figs. 2 and 6).

To highlight the presence of a zero-differential resistance state (ZDRS), we have calculated the dependence of $V_{\mathrm{nl};L}$ on current by integrating the experimental differential resistance data. The results obtained after this procedure are represented in Fig. 8, which shows that the voltage $V_{\mathrm{nl};L}$ exhibits a plateau at negative $I$ where it is almost independent of current in a wide range of magnetic fields, while for positive currents the voltage dependence is almost Ohmic. The inset in Fig. 8 shows the dependence of the voltage on the magnetic field for several values of current inside the ZDRS plateau. These results confirm that the voltage saturates to a constant value independent of current in this regime. The value of the saturation voltage grows almost linearly with magnetic field with weak oscillations that are probably related to the Shubnikov–de Haas oscillations in the longitudinal resistance.

The observed zero-differential state possesses the symmetry of an edge effect. It appears only for the sign of the magnetic field, which ensures that it guides toward the voltage probe electrodes from the distant current sources, and for a specific

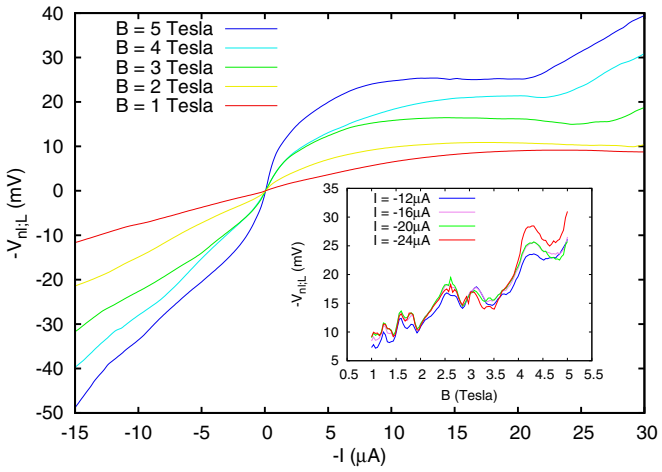


FIG. 8. (Color online) Nonlocal voltage/current characteristics $V_{\mathrm{nl};L}(I)$ for the $\mu = 3\times10^6$ cm$^2$/V s mobility sample at several magnetic fields (for resemblance with data from ZDRS experiments in local geometries, we have shown $-V_{\mathrm{nl};L}$ as a function of $-I$ in this figure). The inset shows the voltage as a function of magnetic field for several currents inside the plateau regime. Temperature was $T = 0.3$ K.

sign of the dc current that creates a voltage drop along the edge tending to stabilize propagation along edges. Therefore, it seems likely that an edge-transport-related mechanism leads to the formation of ZDRS in this case. In the higher-mobility sample where the dimension of the voltage probes was smaller than the mean free path, negative values of NLDR were observed (see Figs. 3 and 6), which suggests that ZDRS is formed due to the clamping of the potential on large length scales by the voltage probe electrodes. On the contrary, if the electrodes are not invasive, the potential exhibits sharp variations whenever the energy of the electrons propagating along the edge is changed by an amount close to $\hbar\omega_c$. These voltage oscillations are probably indicative of a spatially modulated charge-density distribution, and they could explain the observation of oscillating/negative differential resistances in our experiments. It would be highly interesting to understand the role played by the edge mediated ZDRS mechanism in ZDRS experiments realized in the conventional longitudinal resistance measurement geometry.

We note that additional experimental and theoretical investigations are needed to fully understand edge transport at high Landau levels in the nonlinear regime. It would also be interesting to perform similar experiments under microwave irradiation where stabilization of edge channels is expected [32] and where nonlocal effects can also be present [25].

## IV. CONCLUSIONS

To summarize, we have demonstrated through nonlocal resistance measurements that guiding effects can strongly modify the potential distribution in ultrahigh-mobility samples even in the limit of weak magnetic fields, $B \leqslant 0.1$ T. In the linear transport regime, our observations are consistent with a spreading of the distribution of the current source in the direction of propagation along edges. As opposed to the quantum Hall regime, where transport in the bulk is suppressed, an exchange between edge and bulk conduction paths takes place in our experiments. We show that this exchange can be controlled by the amplitude of the potential drop along the edge. Additional edge channels can be formed if the electrons gain energy as they propagate along the edge; in the opposite case when electron lose energy, the edge channels can escape to the bulk. We propose that oscillations in nonlinear transport when the amplitude of the voltage drop along the edge is changed by the spacing between Landau levels are a signature of quantized escape and the formation of edge channels. We also demonstrated that these oscillations develop into zero-differential resistance states when the voltage is clamped on a macroscopic length scale by macroscopic contacts. Thus edge transport in the limit of high filling factors allows us to explore a rich physical regime that may have deep implications in our understanding of electron transport in ultraclean two-dimensional systems.

## ACKNOWLEDGMENTS

We thank M. Polianski and I. A. Dmitriev for fruitful discussions, and we acknowledge support from E. Oppenheimer Foundation, St. Catharine College, and Toshiba Research Europe.

## APPENDIX: CONTINUUM THEORY

In this appendix, we provide a more detailed derivation of formulas from continuum theory that we used in the first section. We start our calculations from the potential created by a point source of current $I$ located at $z = 0$ in a semi-infinite two-dimensional electron gas. It is convenient to represent points in the 2DEG as complex numbers $z = x + iy$, where $(x,y)$ are the point Cartesian coordinates, and the half-plane fills the space $y > 0$. In this case, we find the potential $V_p(z) = R_p(z)I$ with

$$R_p(z) = \frac{\rho_{xx}}{\pi}(\log|z| + \alpha \arg z), \tag{A1}$$

where we have introduced the Hall angle $\alpha = \frac{\rho_{xx}}{\rho_{xy}}$.

A stripe geometry described by $z = x + iy$ with $y \in (0,W)$ can be mapped onto this half-plane using the conformal mapping $z = \exp(\frac{\pi z}{W})$. This allows us to find the potential $V_-(z,x_0) = R_-(z,x_0)I$ created by a point source located on the bottom edge of the stripe at $z = x_0$ ($x_0$ real):

$$V_-(z,x_0) = R_p\left[\exp\left(\frac{\pi z}{W}\right)\exp\left(\frac{-\pi x_0}{W}\right) - 1\right]I. \tag{A2}$$

The potential $V_+(z,x_0) = R_+(z,x_0)I$ created by a source on the top edge of the stripe at $z = x_0 + iW$ reads

$$V_+(z,x_0) = R_p\left[\exp\left(\frac{\pi z}{W}\right)\exp\left(\frac{-\pi x_0}{W}\right) + 1\right]I. \tag{A3}$$

Subtracting these two expressions, we find the potential $V = V_+(z,0) - V_-(z,0)$ created by a current between point-like sources and drains located opposite to each other along the channel (at $z = iW$ and $z = 0$, respectively). For the

particular case of the potential generated along the top edge $y = iW$, far from the sources $|x| \gg W$, we find the following expression:

$$V(x) = \frac{2}{\pi} I \rho_{xx} \exp\left(\frac{-\pi|x|}{W}\right) - \rho_{xy} I \eta(-x), \tag{A4}$$

where $\eta(x)$ is the Heaviside function. This gives the expression for the nonlocal resistance given in the main text:

$$R_{\rm nl} = \frac{2\rho_{xx} D_x}{W} \exp\left(-\frac{\pi L}{W}\right), \tag{A5}$$

where $D_x$ is the spacing between the voltage probes and $L$ is their distance from the source along the channel (for simplicity, we have assumed $D_x \ll W$).


[1] M. Büttiker, Phys. Rev. Lett. **57**, 1761 (1986); M. L. Polianski and M. Büttiker, Phys. Rev. B **76**, 205308 (2007).

[2] A. D. Benoit, C. P. Umbach, R. B. Laibowitz, and R. A. Webb, Phys. Rev. Lett. **58**, 2343 (1987).

[3] P. Cadden-Zimansky and V. Chandrasekhar, Phys. Rev. Lett. **97**, 237003 (2006).

[4] H. van Houten, C. W. J. Beenakker, J. G. Williamson, M. E. I. Broekaart, P. H. M. van Loosdrecht, B. J. van Wees, J. E. Mooij, C. T. Foxon, and J. J. Harris, Phys. Rev. B **39**, 8556 (1989).

[5] N. Kim, J. Kim, J.-O. Lee, K. Kang, K.-H. Yoo, J. W. Park, H.-W. Lee, and J.-J. Kim, J. Phys. Soc. Jpn. **70**, 789 (2001).

[6] P. L. McEuen, A. Szafer, C. A. Richter, B. W. Alphenaar, J. K. Jain, A. D. Stone, R. G. Wheeler, and R. N. Sacks, Phys. Rev. Lett. **64**, 2062 (1990).

[7] A. K. Geim, P. C. Main, P. H. Beton, P. Streda, L. Eaves, C. D. W. Wilkinson, and S. P. Beaumont, Phys. Rev. Lett. **67**, 3014 (1991).

[8] S. Komiyama, Y. Kawaguchi, T. Osada, and Y. Shiraki, Phys. Rev. Lett. **77**, 558 (1996).

[9] Y. Ji, Y. Chung, D. Sprinzak, M. Heiblum, D. Mahalu, and H. Shtrikman, Nature **422**, 415 (2003).

[10] C. Altimiras, H. le Sueur, U. Gennser, A. Cavanna, D. Mailly, and F. Pierre, Nat. Phys. **6**, 34 (2010).

[11] K. Lai, W. Kundhikanjana, M. A. Kelly, Z.-X. Shen, J. Shabani, and M. Shayegan, Phys. Rev. Lett. **107**, 176809 (2011).

[12] E. Bocquillon, F. D. Parmentier, C. Grenier, J.-M. Berroir, P. Degiovanni, D. C. Glattli, B. Plaçais, A. Cavanna, Y. Jin, and G. Fève, Phys. Rev. Lett. **108**, 196803 (2012).

[13] R. G. Mani, J. H. Smet, K. von Klitzing, V. Narayanamurti, W. B. Johnson, and V. Umansky, Nature (London) **420**, 646 (2002).

[14] M. A. Zudov, R. R. Du, L. N. Pfeiffer, and K. W. West, Phys. Rev. Lett. **90**, 046807 (2003).

[15] S. I. Dorozhkin, JETP Lett. **77**, 577 (2003).

[16] R. G. Mani, J. H. Smet, K. von Klitzing, V. Narayanamurti, W. B. Johnson, and V. Umansky, Phys. Rev. Lett. **92**, 146801 (2004).

[17] S. A. Studenikin, M. Potemski, P. T. Coleridge, A. S. Sachrajda, and Z. R. Wasilewski, Solid State Commun. **129**, 341 (2004).

[18] J. H. Smet, B. Gorshunov, C. Jiang, L. Pfeiffer, K. West, V. Umansky, M. Dressel, R. Meisels, F. Kuchar, and K. von Klitzing, Phys. Rev. Lett. **95**, 116804 (2005).

[19] A. A. Bykov, A. K. Bakarov, D. R. Islamov, and A. I. Toropov, JETP Lett. **84**, 391 (2006).

[20] S. Wiedmann, G. M. Gusev, O. E. Raichev, T. E. Lamas, A. K. Bakarov, and J. C. Portal, Phys. Rev. B **78**, 121301(R) (2008).

[21] D. Konstantinov and K. Kono, Phys. Rev. Lett. **105**, 226801 (2010).

[22] M. Khodas, H.-S. Chiang, A. T. Hatke, M. A. Zudov, M. G. Vavilov, L. N. Pfeiffer, and K. W. West, Phys. Rev. Lett. **104**, 206801 (2010).

[23] I. V. Andreev, V. M. Muravev, I. V. Kukushkin, S. Schmult, and W. Dietsche, Phys. Rev. B **83**, 121308(R) (2011).

[24] A. N. Ramanayaka, R. G. Mani, J. Iñarrea, and W. Wegscheider, Phys. Rev. B **85**, 205315 (2012).

[25] D. Konstantionv, A. D. Chepelianskii, and K. Kono, J. Phys. Soc. Jpn. **81**, 093601 (2012).

[26] R. G. Mani, A. N. Ramanayaka, T. Ye, M. S. Heimbeck, H. O. Everitt, and W. Wegscheider, Phys. Rev. B **87**, 245308 (2013).

[27] D. Konstantinov, Y. Monarkha, and K. Kono, Phys. Rev. Lett. **111**, 266802 (2013).

[28] I. A. Dmitriev, A. D. Mirlin, D. G. Polyakov, and M. A. Zudov, Rev. Mod. Phys. **84**, 1709 (2012).

[29] A. A. Bykov, J.-q. Zhang, S. Vitkalov, A. K. Kalagin, and A. K. Bakarov, Phys. Rev. Lett. **99**, 116801 (2007).

[30] A. T. Hatke, H.-S. Chiang, M. A. Zudov, L. N. Pfeiffer, and K. W. West, Phys. Rev. B **82**, 041304(R) (2010).

[31] A. A. Bykov, S. Byrnes, S. Dietrich, S. Vitkalov, I. V. Marchishin, and D. V. Dmitriev, Phys. Rev. B **87**, 081409(R) (2013).

[32] A. D. Chepelianskii and D. L. Shepelyansky, Phys. Rev. B **80**, 241308(R) (2009).

[33] A. D. Chepelianskii, J. Laidet, I. Farrer, H. E. Beere, D. A. Ritchie, and H. Bouchiat, Phys. Rev. B **86**, 205108 (2012).

[34] O. V. Zhirov, A. D. Chepelianskii, and D. L. Shepelyansky, Phys. Rev. B **88**, 035410 (2013).

[35] S. A. Mikhailov, Phys. Rev. B **89**, 045410 (2014); the theory in this reference concentrates on the role of contact effects, however it invokes edge transport effects to explain the influence of the contacts on the four terminal resistance.

[36] A. D. Levin, Z. S. Momtaz, G. M. Gusev, and A. K. Bakarov, Phys. Rev. B **89**, 161304(R) (2014).

[37] Y. Avishai and G. Montambaux, Eur. Phys. J. B **66**, 41 (2008).

[38] C. W. J. Beenakker and H. van Houten, Phys. Rev. Lett. **63**, 1857 (1989).

[39] P. Svoboda, P. Streda, G. Nachtwei, A. Jaeger, M. Cukr, and M. Láznicka, Phys. Rev. B **45**, 8763 (1992).

[40] A. H. MacDonald, T. M. Rice, and W. F. Brinkman, Phys. Rev. B **28**, 3648 (1983).

[41] O. Heinonen and M. D. Johnson, Phys. Rev. B **49**, 11230 (1994).